

**$\mathcal{O}(\Gamma)$  Corrections to  $W$  pair production  
in  $e^+e^-$  and  $\gamma\gamma$  collisions**Andre Aeppli<sup>a†</sup>  
Frank Cuypers<sup>b</sup>  
Geert Jan van Oldenborgh<sup>c</sup><sup>a</sup> *Institut für Theoretische Teilchenphysik  
Universität Karlsruhe**Kaiserstr. 12, D-7500 Karlsruhe 1, Germany*<sup>b</sup> *Sektion Physik der Universität München,  
Theresienstraße 37, D-8000 München 2, Germany*<sup>c</sup> *Paul Scherrer Institut, CH-5232 Villigen PSI, Switzerland***Abstract**

Several schemes to introduce finite width effects to reactions involving unstable elementary particles are given and the differences between them are investigated. The effects of the different schemes is investigated numerically for  $W$  pair production. In  $e^+e^- \rightarrow W^+W^-$  we find that the effect of the non-resonant graphs cannot be neglected for  $\sqrt{s} \geq 400$  GeV. There is no difference between the various schemes to add these to the resonant graphs away from threshold, although some violate gauge invariance. On the other hand, in the reaction  $\gamma\gamma \rightarrow W^+W^-$  the effect of the non-resonant graphs is large everywhere, due to the  $t$ -channel pole. However, even requiring that the outgoing lepton is observable ( $p_{\perp} > .02\sqrt{s}$ ) reduces the contribution to about 1%. Again, the scheme dependence is negligible here.

†Supported by BMFT Grant No. 055KAP94P1

# 1 Introduction

Although a general treatment of unstable particles in quantum field theory has been given a long time ago [1], the technical difficulties especially in the context of gauge invariance are considerable and need careful investigations. Recently, several authors [2, 3, 4] proposed a gauge invariant procedure to include consistently higher order corrections at the  $Z$  pole. As an example of a 2-resonance production process, finite width effects up to one-loop have been calculated for  $e^+e^- \rightarrow ZZ$  [5]. Here we will present a computation of the tree level cross section for  $W$ -pair production in various schemes. This reaction introduces two new elements: non-resonant diagrams can not be separated from the resonance production diagrams in a gauge invariant way, and (in contrast to the case of  $Z$  pair production) large unitarity cancellations are present in  $e^+e^-$  collisions, which may dramatically enhance gauge violating terms in the cross section.

The differences between these various schemes constitute the  $\mathcal{O}(\Gamma)$  corrections to the reaction. Note that these are formally of the same order as the one-loop corrections ( $\Gamma/M \propto \alpha$ ), and these must thus be combined properly. This will be the subject of a forthcoming paper [6].

We compare several methods used to compute the off-shell effects, some of which are gauge variant or have unacceptable properties near threshold. Next we consider what the practical implications are for the total cross section of  $W$  pair production, both at LEP II and at future linear  $e^+e^-$  and  $\gamma\gamma$  colliders. (The latter are constructed out of an  $e^-e^-$  collider by Compton scattering of an intense laser beam [7].) In many channels  $W$  pair production is the major source of events, either as a signal to study the properties of the  $W$  boson [8] or as background to more exotic processes [9]. In both cases a thorough understanding of the standard model prediction is required.

The layout of this paper is as follows. In section 2 we list the various schemes that can be used to evaluate cross sections for reactions involving (charged) unstable elementary particles, and their shortcomings. Next we perform this calculation for  $e^+e^- \rightarrow W^+W^-$  (section 3) and  $\gamma\gamma \rightarrow W^+W^-$  (section 4), discussing the applicability of the various approximations.

## 2 Methods

There are various methods to compute the cross sections for reactions involving unstable particles. We will give a list of these, with discussions of their merits, in this section. For simplicity we first discuss the schemes for a single unstable particle and give the extension to two particles later. The prototypical reaction will be  $e^+e^- \rightarrow W^+\mu^-\bar{\nu}_\mu$  with the  $W^+$  considered stable.

The first approximation to a process whose leading contributions factorizes into the production and decay of unstable particles is the narrow width approximation. One treats the unstable particles as stable in a production cross

section and multiplies with the relevant branching ratios, obtaining

$$\begin{aligned}\sigma_{\text{NWA}} &= \frac{1}{2s} \int dPS_{e^+e^- \rightarrow W^+W^-} |\mathcal{M}_{e^+e^- \rightarrow W^+W^-}|^2 \times \frac{\Gamma_{W^- \rightarrow \mu^- \nu_\mu}}{\Gamma_W} \\ &= \frac{1}{2s} \int dPS_{e^+e^- \rightarrow W^+W^- \rightarrow \mu^- \bar{\nu}_\mu} |\mathcal{M}_{e^+e^- \rightarrow W^+W^-}|^2 \times \frac{|M_{W^- \rightarrow \mu^- \nu_\mu}|^2}{2m_W \Gamma_W} \end{aligned} \quad (1)$$

where  $dPS_{ab \rightarrow cd}$  denotes the phase space element.

This fails to take into account terms of  $\mathcal{O}(\Gamma)$ ; the corresponding dimensionless parameter will usually be  $\Gamma/m$  (about 1/40 for the  $W$ ), but can be  $m^3\Gamma/\lambda(s, m_1^2, m_2^2)$  near a threshold for the production of particles 1 and 2 in the expansion of the phase space factor  $\sqrt{\lambda}$ . The narrow width approximation is not defined below the threshold for production of the unstable particle.

Above threshold the most important of these  $\mathcal{O}(\Gamma)$  corrections are included by simply using the on-shell expression for the matrix element, but treating the kinematics and unstable particle propagator off-shell. This off-shell propagator is derived by resumming the one-loop corrections to the propagator, giving rise to a simple Breit-Wigner propagator  $1/(p^2 - m^2 + im\Gamma)$  with  $\Gamma$  defined by the relation<sup>1</sup>  $m\Gamma = \text{Im}\Pi(m^2)$  in terms of the self energy  $\Pi$ . We refer to this procedure as the ‘‘resonant’’ scheme:

$$\sigma_{\text{res}} = \frac{1}{2s} \int dPS_{e^+e^- \rightarrow W^+\mu^- \bar{\nu}_\mu} \frac{|\mathcal{M}_{e^+e^- \rightarrow W^+W^-}|^2 \times |M_{W^- \rightarrow \mu^- \nu_\mu}|^2}{(p_{W^-}^2 - m_W^2)^2 + m_W^2 \Gamma_W^2}. \quad (2)$$

The amplitude thus has the form

$$\mathcal{M}_{\text{res}} = \frac{R(m_W^2, \theta_i)}{p_{W^-}^2 - m_W^2 + im_W \Gamma_W}, \quad (3)$$

where  $R(p_{W^-}^2, \theta_i)/(p_{W^-}^2 - m_W^2)$  denotes the amplitude resulting from the resonant diagrams, i.e. those diagrams which contain a  $W$  which can be on-shell in the kinematically allowed region. (These are given in Fig. 1 for the full process.) The essential variable in this amplitude is the virtuality  $p_{W^-}^2$  of the  $W^-$ . The other kinematical variables are assumed to be angles, which are independent of  $p_{W^-}^2$ . We will suppress them from now on. It can easily be verified that the narrow width approximation follows from the limit  $\Gamma \rightarrow 0$  in Eq. (2). Below threshold the resonant cross section is zero, as  $R(m_W^2) = 0$ .

The next step is usually to also evaluate the matrix element off-shell, thus to use an amplitude

$$\mathcal{M}_{\text{off}} = \frac{R(p_{W^-}^2)}{p_{W^-}^2 - m_W^2 + im_W \Gamma_W}; \quad (4)$$

we refer to this procedure as the ‘‘off-shell’’ method. This also gives an answer below threshold. In the case of a charged resonance however, this procedure violates  $U(1)_{em}$ -gauge invariance, even if the width is given by the physical

<sup>1</sup> This approximation may not be sufficient in the threshold region and can be replaced by an  $s$ -dependent expression of the form  $m\Gamma \rightarrow s\Gamma/m$ .

(on-shell) quantity, which is gauge invariant. The reason is that the original resonant graphs are not the only graphs which lead to the particular final state: non-resonant graphs (like those of Fig. 2) have to be included. Only the sum of these graphs is gauge invariant for  $p_{W^-}^2 \neq m_W^2$  and an unresummed unstable particle propagator.

The “naive” way to include these non-resonant graphs is to just add them with a complex mass:

$$\mathcal{M}_{\text{naive}} = \frac{R(p_{W^-}^2)}{p_{W^-}^2 - m_W^2 + im_W\Gamma_W} + N(p_{W^-}^2), \quad (5)$$

where  $N(p_{W^-}^2)$  denotes the contribution from the non-resonant graphs. However, as the amplitude was gauge invariant for  $\Gamma_W = 0$  it follows that it must be gauge variant for  $\Gamma_W > 0$  (if the resonant graphs are not separately gauge invariant). We will discuss the size of these gauge breaking terms at the end of this section.

An obviously gauge invariant procedure to include the non-resonant graphs was introduced by Zeppenfeld *et al.* [10]. There, resonant and non-resonant terms are multiplied by the common factor  $(p^2 - m^2)/(p^2 - m^2 + im\Gamma)$ :

$$\mathcal{M}_{\text{all}} = \frac{R(p_{W^-}^2)}{p_{W^-}^2 - m_W^2 + im_W\Gamma_W} + \frac{p^2 - m^2}{p^2 - m^2 + im\Gamma} N(p_{W^-}^2), \quad (6)$$

The price to save gauge invariance in this “overall” scheme is of course an incorrect treatment of the non-resonant contribution close to mass shell. However, it can be argued that here the difference is of higher order in this region of phase space. We thus have a prescription which is correct to leading order both on resonance and away from it, but these contributions are formally of different order in  $\alpha$ . Still, when the non-resonant graphs are large this may be a sensible approximation.

Another gauge invariant way to include the off-shell effects is to systematically separate orders in  $\Gamma$ . A similar procedure was used for instance in Ref. [2] to include the higher-order corrections at the  $Z$ -pole correctly. In this “polescheme” the matrix element has the form

$$\mathcal{M}_{\text{pole}} = \frac{R(m_W^2)}{p_{W^-}^2 - m_W^2 + im_W\Gamma_W} + [\tilde{R}(p_{W^-}^2) + N(p_{W^-}^2)] \quad (7)$$

with

$$\tilde{R}(p_{W^-}^2) = \frac{R(p_{W^-}^2) - R(m_W^2)}{p_{W^-}^2 - m_W^2} \quad (8)$$

As the residue at the pole  $p_{W^-}^2 = m_W^2$  is gauge invariant one can add the finite width in the first term without breaking gauge invariance. This corresponds to adding and resumming only the gauge invariant part of the propagator corrections. In this scheme the cross section is given as the sum of the resonant cross section plus  $\mathcal{O}(\Gamma)$  corrections, which are both gauge invariant. (The half-resonant term  $2\text{Re}[R^\dagger(m_W^2)(\tilde{R}(p_{W^-}^2) + N(p_{W^-}^2))]/(p_{W^-}^2 - m_W^2 + im_W\Gamma_W)$ ) and

the non-resonant term  $|\tilde{R}(p_{W-}^2) + N(p_{W-}^2)|^2$  are of the same order in  $\Gamma_W$  after integration over  $p_{W-}^2$ . It is thus a natural starting point for higher order corrections. A detailed discussion on the one-loop corrections will be given in a Ref. [6].

However, the polescheme also has some undesirable properties. The first (resonant) term has a discontinuity when the threshold for the production of the unstable particle is crossed. Approaching from below, one even encounters the original (non-resummed) singularity in the propagator. The accuracy of this scheme is thus doubtful around threshold.

Below threshold we thus have the following unsatisfactory situation: the narrow width scheme is undefined; the resonant cross section is zero and the polescheme diverges. The other schemes give a finite answer, but are otherwise flawed. It may be surmised that the problems in the threshold region can be traced back to the low momenta of the  $W$  bosons there, which have time to exchange photons. One does thus not expect a lowest order or one-loop computation to give a reliable answer. A bound-state calculation (as recently performed for top production [11]) or resummation of the resulting ladder graphs looks necessary here.

The extensions for reactions with two unstable particles in the final state are largely straightforward. One now finds not only graphs of  $\mathcal{O}(\Gamma)$  but also of  $\mathcal{O}(\Gamma^2)$ ; the doubly non-resonant graphs. In the case of  $e^+e^- \rightarrow 4$  fermions, these are only present when there are electrons in the final state. In  $\gamma\gamma$  collisions they are always present. In the polescheme one can systematically neglect these graphs; in the case of two similar particles like  $W^+W^-$  the  $\mathcal{O}(\Gamma)$  corrections are just two times the size of the corrections to the process with one particle regarded unstable<sup>2</sup>.

Below threshold one has to be very careful in the polescheme; in case of the production of two identical particles (and nothing else) can one regain a finite expression by symmetrizing:

$$\begin{aligned} \sigma = & \int dPS_{e^+e^- \rightarrow 4 \text{ fermions}} \frac{\theta(p_{W-}^2 - p_{W+}^2)}{p_{W+}^2 - m_W^2} \left| \frac{R(p_{W+}^2, m_W^2)}{p_{W-}^2 - m_W^2 + im_W\Gamma_W} \right. \\ & \left. + \frac{R(p_{W+}^2, p_{W-}^2) - R(p_{W+}^2, m_W^2)}{p_{W-}^2 - m_W^2} + N(p_{W+}^2, p_{W-}^2) \right|^2 + (W^+ \leftrightarrow W^-) \end{aligned} \quad (9)$$

Of course this expression still diverges as  $s \rightarrow 4m_W^2$ .

Finally, we compute the order of the difference between the three schemes that include the non-resonant graphs. The difference between the ‘‘overall’’ scheme and the polescheme in the matrix element squared is

$$\begin{aligned} |\mathcal{M}_{\text{pole}}|^2 - |\mathcal{M}_{\text{all}}|^2 = & -2m_W\Gamma_W \frac{\text{Im}\left(R^\dagger(m_W^2)[\tilde{R}(p_{W-}^2) + N(p_{W-}^2)]\right)}{(p_{W-}^2 - m_W^2)^2 + m_W^2\Gamma_W^2} \\ & + m_W^2\Gamma_W^2 \frac{\left|\tilde{R}(p_{W-}^2) + N(p_{W-}^2)\right|^2}{(p_{W-}^2 - m_W^2)^2 + m_W^2\Gamma_W^2} \end{aligned} \quad (10)$$

---

<sup>2</sup>If the decay products are treated identically experimentally.

The first term, which is of  $\mathcal{O}(\Gamma)$  relative to the resonant term, is proportional to the Levi-Civita tensor  $\epsilon_{\mu\nu\rho\sigma}p_1^\mu p_2^\nu p_3^\rho p_4^\sigma$ , with the  $p_i^\mu$  four independent momenta. This term will disappear when integrated over a set of reasonably symmetric cuts<sup>3</sup>. Note that this is not the case in general in doubly differential cross sections. The second term is of  $\mathcal{O}(\Gamma^2)$  and thus negligible in our approximations.

The difference between the gauge variant “naive” formulation and the polescheme is given by

$$\begin{aligned}
|\mathcal{M}_{\text{pole}}|^2 - |\mathcal{M}_{\text{naive}}|^2 &= 2m_W\Gamma_W \frac{\text{Im}\left((p_{W^-}^2 - m_W^2)\tilde{R}^\dagger(p_{W^-}^2)N(p_{W^-}^2) - R^\dagger(m_W^2)\tilde{R}(p_{W^-}^2)\right)}{(p_{W^-}^2 - m_W^2)^2 + m_W^2\Gamma_W^2} \\
&\quad + m_W^2\Gamma_W^2 \frac{\left|\tilde{R}(p_{W^-}^2)\right|^2 + 2\text{Re}\left(\tilde{R}^\dagger(p_{W^-}^2)N(p_{W^-}^2)\right)}{(p_{W^-}^2 - m_W^2)^2 + m_W^2\Gamma_W^2} \quad (11)
\end{aligned}$$

Again, the  $\mathcal{O}(\Gamma)$  term will disappear when integrated over a symmetric part of phase space, and the difference (including the gauge breaking terms) are of order  $\Gamma^2$ .

A summary of the six different schemes we have defined in this section and their properties can be found in table 1.

### 3 $e^+e^- \rightarrow W^+W^-$

Depending on the cm energy  $\sqrt{s}$  of this reaction, two complementary aspects of the problem are revealed. Even at highest possible LEP II energies [12] the inherent unitarity cancellations are at most of the order of a few percent of the total cross section whereas the effect of the  $W$ -width amounts to more than 10%. Testing the Standard model predictions within reasonable limits at LEP II requires therefore an accuracy of the calculations below 1% and thus a detailed analysis of the width effects. On the other hand at energies  $\sqrt{s} \approx 500$  GeV [13] the finite width effect is small but the unitarity cancellations account for more than an order of magnitude. Any gauge breaking term induced by resummation or the omission of non-resonant graphs may thus be enhanced and could upset any prediction of the model.

In the following we will illustrate numerically the general results obtained in the previous section. For definiteness we consider  $e^+e^- \rightarrow u\bar{d}\mu\bar{\nu}_\mu$  in the  $\alpha$ -scheme; therefore we use the fine structure constant  $\alpha$ ,  $M_Z = 91.177$  GeV and correspondingly  $M_W = 80.23$  GeV as input parameters. The value for the  $W$ -width is then  $\Gamma_W = 2.072$  GeV, assuming  $m_t = 140$  GeV and  $m_H = 100$  GeV [14]. We work in the unitary gauge.

The resonant diagrams are the well known s- and t-channel diagrams given in Fig. 1. In addition there are many non-resonant diagrams with essentially 3 different topologies. Imposing appropriate restrictions on the 4 fermion final state (no electrons), only annihilation-type diagrams (like in Fig. 2) contribute. Since the flavor content of the final state does not alter gauge cancellation, it

<sup>3</sup>To be precise, the cuts should not introduce more than one spatial direction other than the beam axis so that there are no more than three independent four vectors after integration.

is clear that diagrams with the other topologies form gauge invariant subsets by themselves. The result for the resonant diagrams using a Breit-Wigner type propagator has been given some time ago [15]. In Ref. [16], the annihilation type non-resonant diagrams has been added. In Fig. 5 we show the results of an explicit calculation of all the schemes discussed so far. Except below threshold, where only some schemes give a non-zero result, and the narrow width approximation near threshold, they all agree to within a few percent. The differences with the doubly resonant cross section are shown in Fig. 6.

The difference between the gauge invariant “overall” scheme and the “naive” results of [16] is completely negligible over this range of  $\sqrt{s}$ , at least in the unitary gauge that we use. The only sizable effect of the non-resonant diagrams is obtained for energies close to threshold and above 400 GeV. Otherwise, taking the resonant diagrams off-shell and ignoring the non-resonant graphs gives a very good description.

The two gauge invariant calculations agree very well down to 180 GeV. At  $\sqrt{s} = 185$  GeV the difference is 0.4%. Closer to threshold the two procedures start deviating significantly. Since the “overall” scheme result mistreats the non-resonant terms, whereas the polescheme is highly discontinuous, we take this difference to indicate our ignorance of the threshold region.

#### 4 $\gamma\gamma \rightarrow W^+W^-$

The resonant and non-resonant Feynman diagrams for the reaction  $\gamma\gamma \rightarrow \ell^- \bar{\nu}_\ell W^+$  are given in Figs 3 and 4 respectively. To restrict ourselves to the  $\mathcal{O}(\Gamma)$  corrections we consider the  $W^+$  stable; otherwise doubly non-resonant diagrams are needed for a gauge invariant result. The total corrections with both  $W$  bosons unstable are about twice the size of the corrections given here. (In the polescheme the factor 2 is exact, up to  $\mathcal{O}(\Gamma^2)$  terms).

This reaction is important at possible future  $\gamma\gamma$  colliders to study the  $WW\gamma$  coupling and as a background to missing  $p_\perp$  physics [9]. The non-resonant diagrams contain large logarithms  $\log(m_\ell^2/s)\Gamma_W/m_W$  in the total cross section (as appear in the similar diagrams for the reaction  $\gamma\gamma \rightarrow e^+e^-Z_0$ ). To suppress these we impose a  $p_\perp$  cut on the outgoing leptons,  $p_\perp(\ell) > 0.02\sqrt{s}$ ; this should give an indication of detector acceptance. With this cut the contribution of the non-resonant diagrams is again very small, about 1% over a large range in  $\sqrt{s}$ . The difference between the different schemes to include these diagrams is negligible, even near threshold. In this calculation we work in the 't Hooft-Feynman gauge.

A more realistic picture is painted in Fig. 9, where we have folded the cross section with the lowest order spectrum resulting from the conversion of the electron beam in a photon beam via Compton scattering [7]. The same conclusions hold here.

## 5 Conclusions

A study has been made of various schemes to handle processes with unstable particles in intermediate states. The application of these schemes in two processes,  $e^+e^- \rightarrow 4$  fermions and  $\gamma\gamma \rightarrow e^-\bar{\nu}_e W^+$  shows that in general the corrections due to the width of the  $W$  boson are small, at least when the phase space is taken off-shell.

As was shown before, for  $e^+e^-$  collisions the non-resonant diagrams become important only at threshold (where the signal is low) and at high energies ( $\sqrt{s} > 500$  GeV). At least in the commonly used gauges we worked in, there is not much difference (less than 0.5%) between the various gauge invariant and gauge variant schemes to include the non-resonant graphs. This violation of  $U(1)_{em}$  gauge invariance is apparently not amplified by the large unitarity cancellations which occur in these processes. Near threshold we encounter some uncertainties.

For  $\gamma\gamma$  collisions the non-resonant graphs contribute much less, after a mild  $p_\perp$  cut. The difference does not amount to much more than 1% over a large range of energies and even close to threshold.

**Acknowledgements** We would like to thank Daniel Wyler and Reinhold Rückl for useful discussions.

## References

- [1] M. Veltman. *Physica* **29** (1963) 186.
- [2] R. G. Stuart. *Phys. Lett.* **B262** (1991) 113.
- [3] A. Sirlin. *Phys. Rev. Lett.* **67** (1991) 2127.
- [4] H. Veltman. DESY 92-076 (1992).
- [5] A. Denner and Th. Sack. *Z. Phys.* **C45** (1990) 439.
- [6] A. Aeppli, G. J. van Oldenborgh and D. Wyler. (to appear).
- [7] I. F. Ginzburg, Kotkin G. L., V. G. Serbo and V. I. Telnov. *Nucl. Instr. Meth.* **205** (1983) 47.
- [8] G. Belanger and F. Boudjema. *Phys. Lett.* **B288** (1992) 210.
- [9] F. Cuypers, G. J. van Oldenborgh and R. Rückl. CERN-TH.6742/92, MPI-Ph/92/73, LMU-92/07 (1992).
- [10] D. Zeppenfeld, J. A. M. Vermaseren and U. Baur. *Nucl. Phys.* **B375** (1992) 3.
- [11] M. Jezabek, J. H. Kuhn and T. Teubner. TTP-92-16.
- [12] Edited by Böhm and W. Hoogland. Proceedings of the ECFA Workshop on LEP 200, Aachen, 1986. ECFA, CERN 87-08.



- [13] Edited by P. M. Zerwas. Proceedings of the Workshop on  $e^+e^-$  collisions at 500 GeV, Munich, Annecy, Hamburg, 1991. DESY 92-123A.
- [14] A. Denner. Habilitations thesis, Univeristy of Würzburg, 1992.
- [15] T. Muta, R. Najima and S. Wakaizumi. Mod. Phys. Lett. **A1** (1986) 203.
- [16] A. Aeppli and D. Wyler. Phys. Lett. **B262** (1991) 125.

## A Table

name	kinematics	matrix element	gauge invariant	threshold behaviour
narrow width	on-shell	$R(m^2)$	yes	undefined below threshold
resonant	off-shell	$\frac{R(m^2)}{p^2 - m^2 + im\Gamma}$	yes	zero below threshold
offshell	off-shell	$\frac{R(p^2)}{p^2 - m^2 + im\Gamma}$	no	wrong below threshold
naive	off-shell	$\frac{R(p^2)}{p^2 - m^2 + im\Gamma} + N(p^2)$	no	ok
overall	off-shell	$\frac{R(m^2)}{p^2 - m^2 + im\Gamma} + \frac{p^2 - m^2}{p^2 - m^2 + im\Gamma} N(p^2)$	yes	ok
polescheme	off-shell	$\frac{R(m^2)}{p^2 - m^2 + im\Gamma} + \tilde{R}(p^2) + N(p^2)$	yes	wrong around threshold

Table 1: A summary of the six different schemes to treat unstable particles defined in section 2

## B Figures

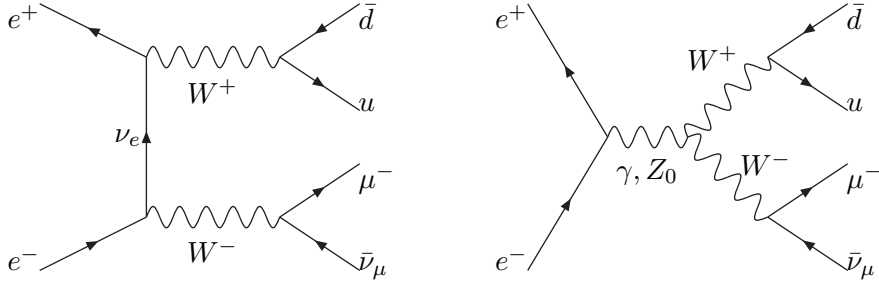


Figure 1: Resonant diagrams for  $e^+e^- \rightarrow \mu^-\bar{\nu}_\mu u\bar{d}$

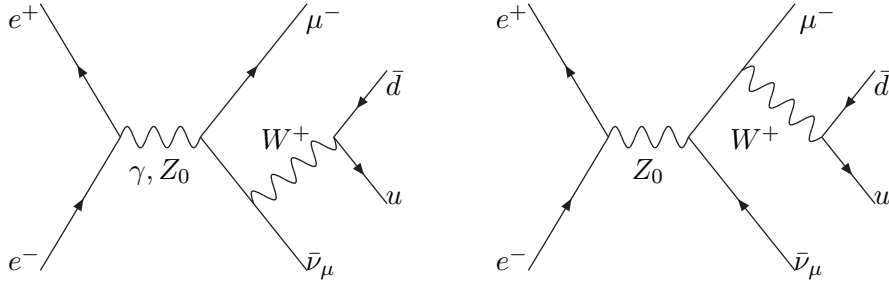


Figure 2: Two of the four non-resonant diagrams for  $e^+e^- \rightarrow \mu^-\bar{\nu}_\mu u\bar{d}$

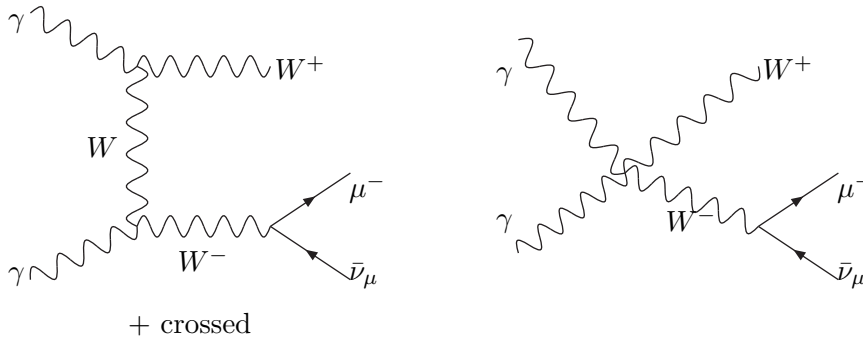


Figure 3: Resonant diagrams for  $\gamma\gamma \rightarrow \ell^-\bar{\nu}_\ell W^+$

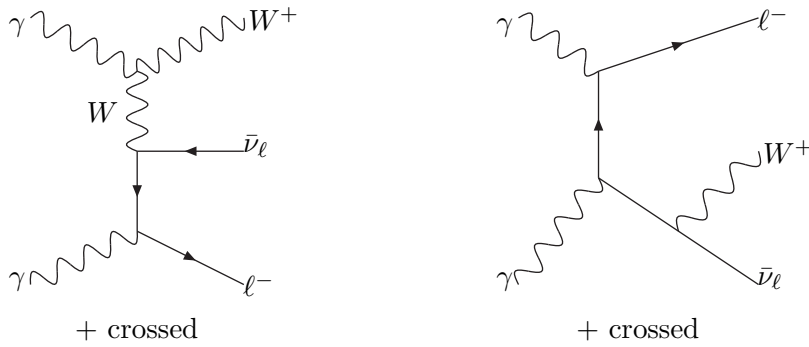


Figure 4: Non-resonant diagrams for  $\gamma\gamma \rightarrow \ell^-\bar{\nu}_\ell W^+$

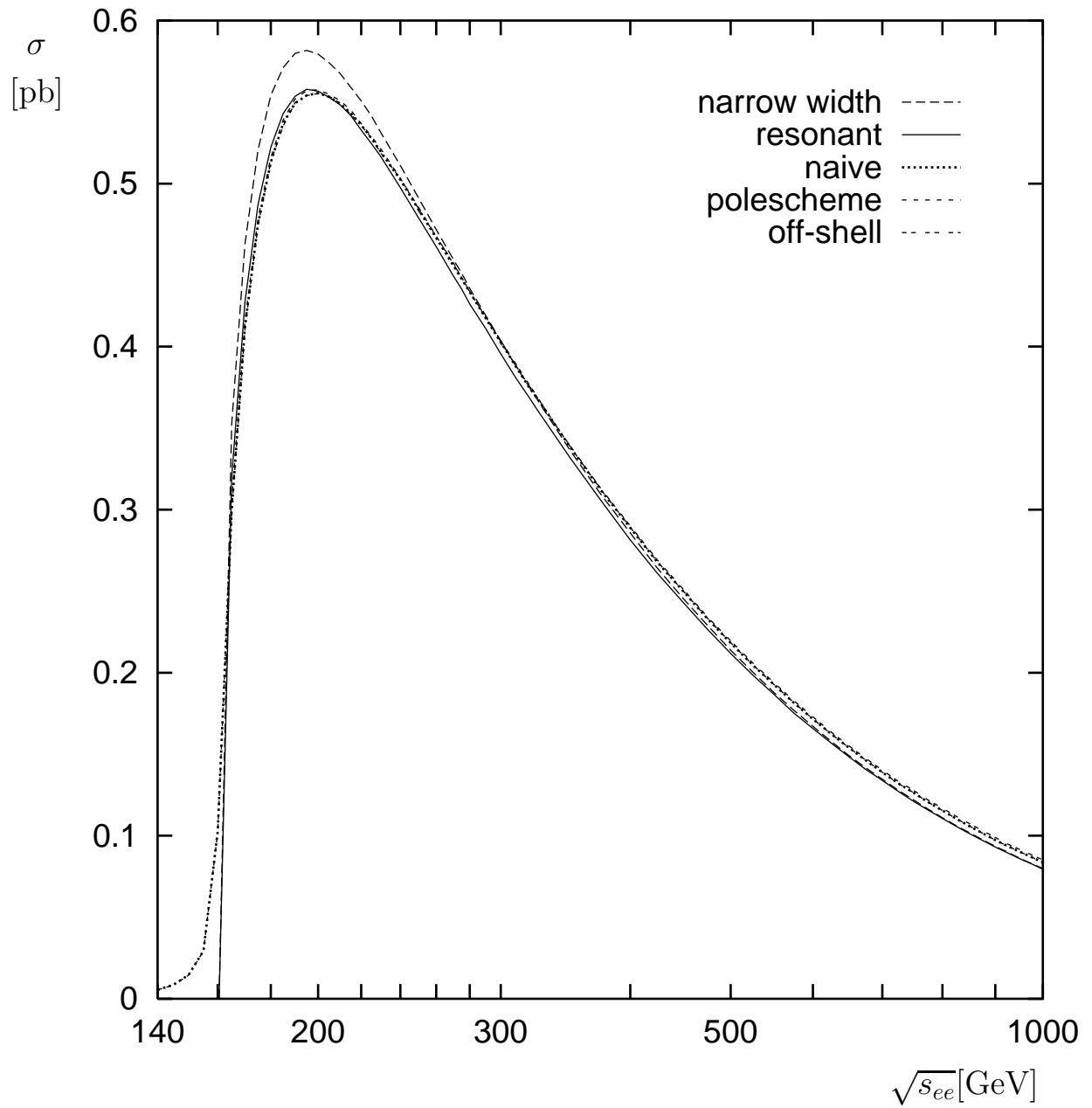


Figure 5: Cross sections for  $e^+e^- \rightarrow \mu^- \bar{\nu}_\mu u \bar{d}$  in the different schemes defined in the text. The “overall” scheme yields results which are indistinguishable from those of the “naive” scheme.

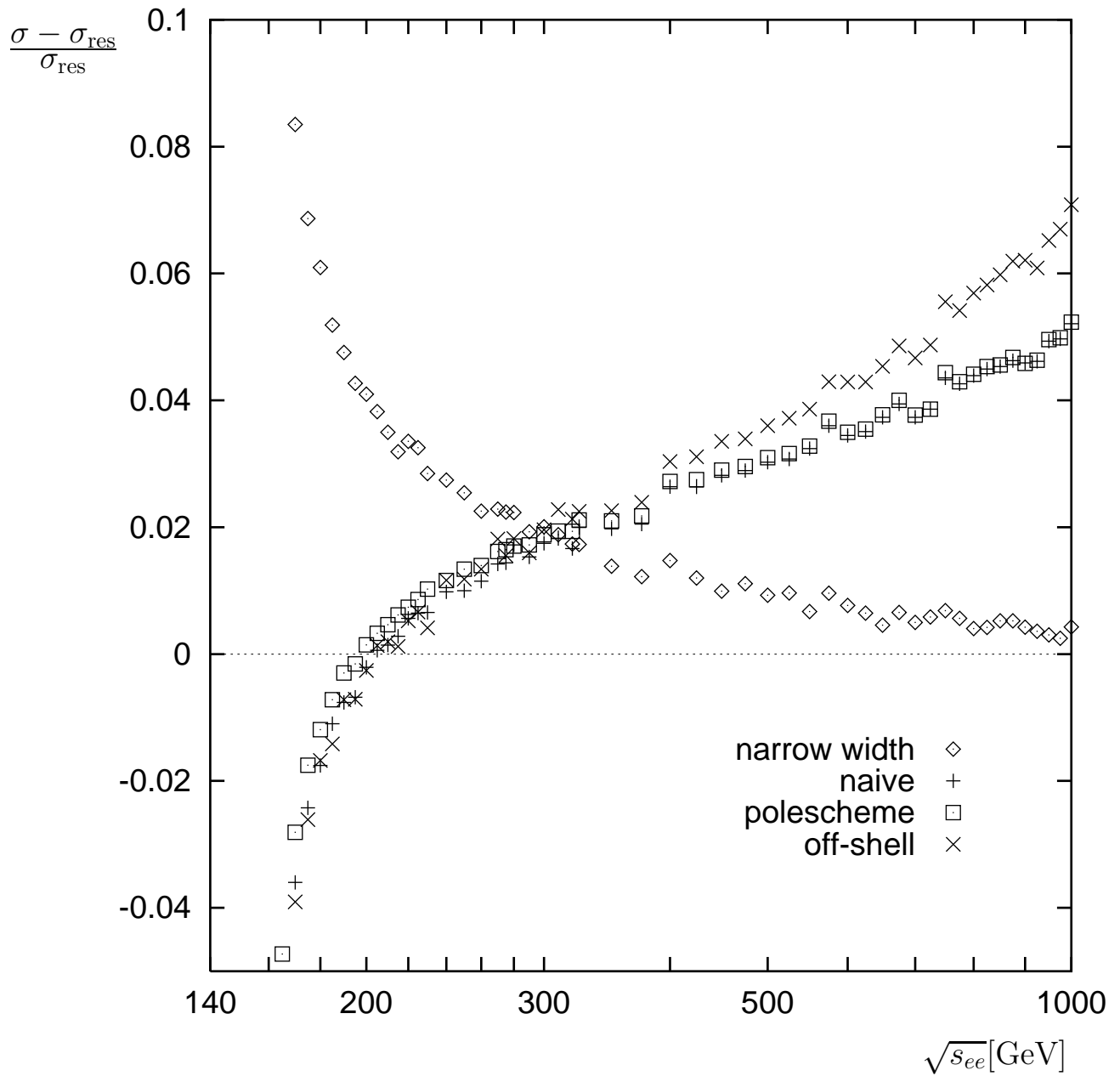


Figure 6: Relative differences with the doubly resonant cross section for  $e^+e^- \rightarrow \mu^-\bar{\nu}_\mu u\bar{d}$ . The scatter is due to limited integration accuracy.

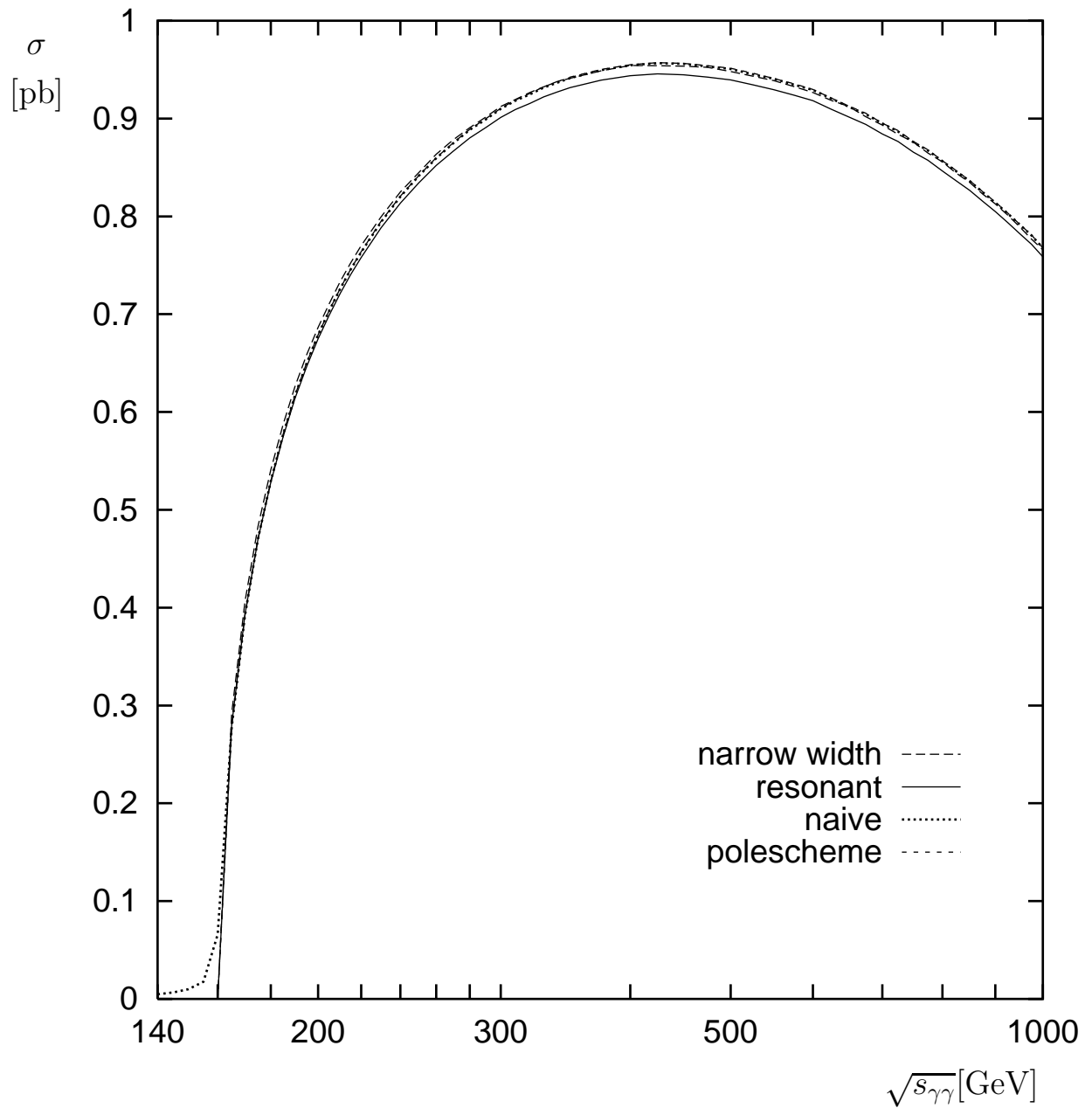


Figure 7: Cross sections for  $\gamma\gamma \rightarrow \ell^- \bar{\nu}_\ell W^+$  in the different schemes defined in the text, with  $p_\perp(\ell) > 0.02\sqrt{s_\gamma}$  and a monochromatic laser beam. The difference between the “naive” and “overall” schemes is again not visible on this plot.

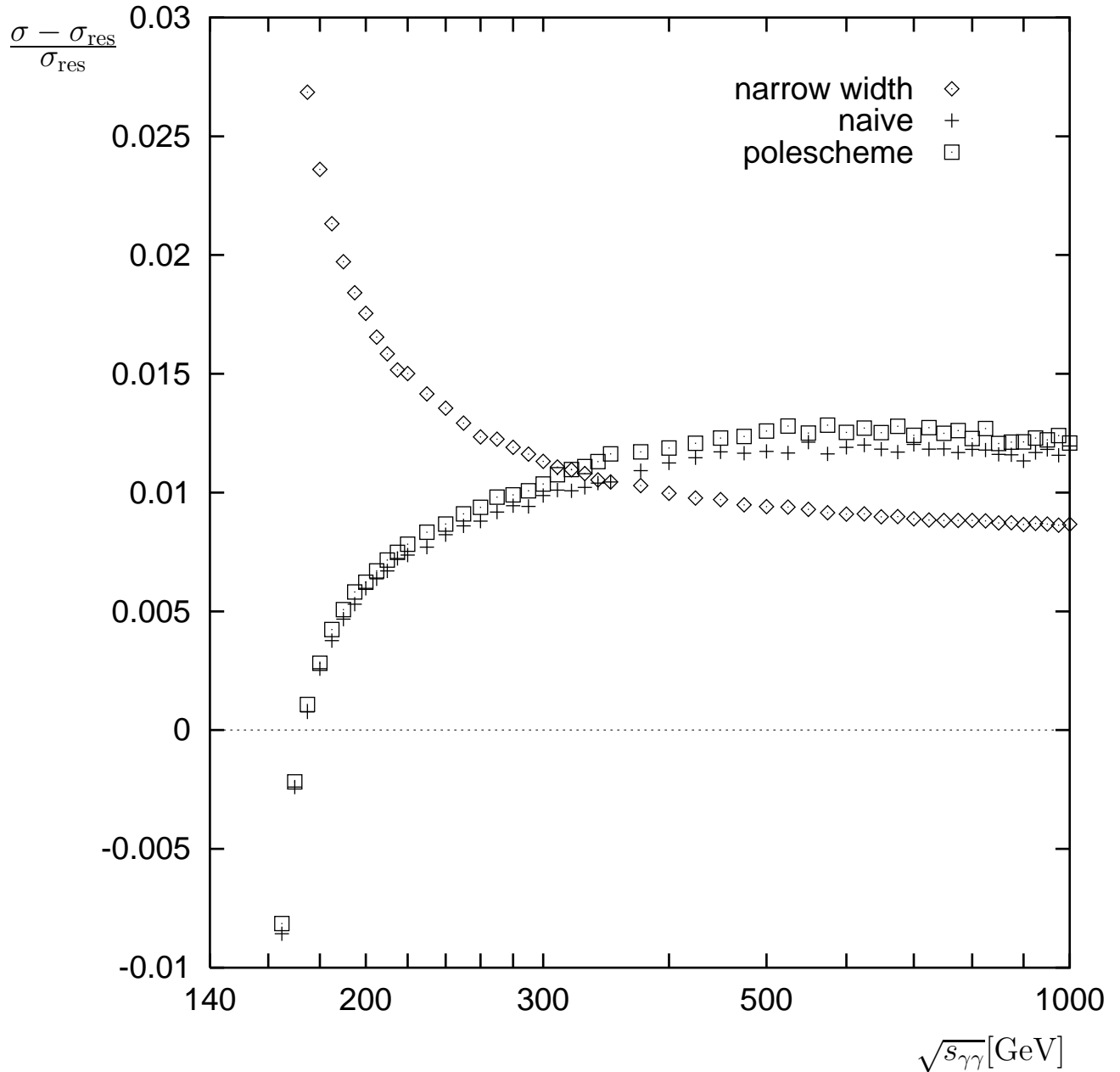


Figure 8: Differences with the doubly resonant cross section for  $\gamma\gamma \rightarrow \ell^- \bar{\nu}_\ell W^+$  as a fraction of the resonant cross section. The full  $\mathcal{O}(\Gamma)$  corrections, including the width of the  $W^+$ , are about twice this size.

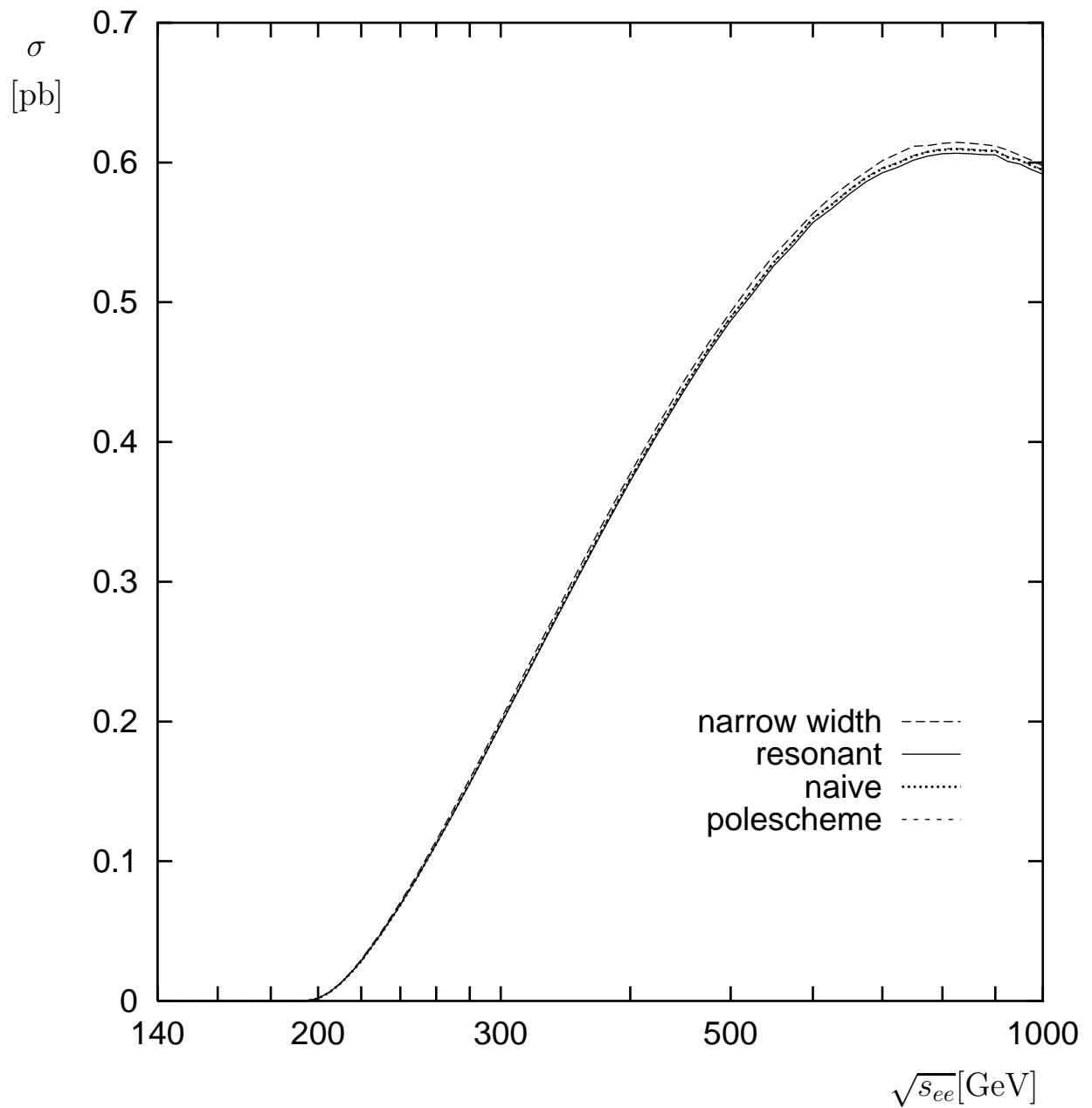


Figure 9: Cross sections for  $\gamma\gamma \rightarrow \ell^- \bar{\nu}_\ell W^+$  in the different schemes defined in the text with a more realistic photon spectrum [7]; again we demand that  $p_\perp(\ell) > 0.02\sqrt{s_{ee}}$



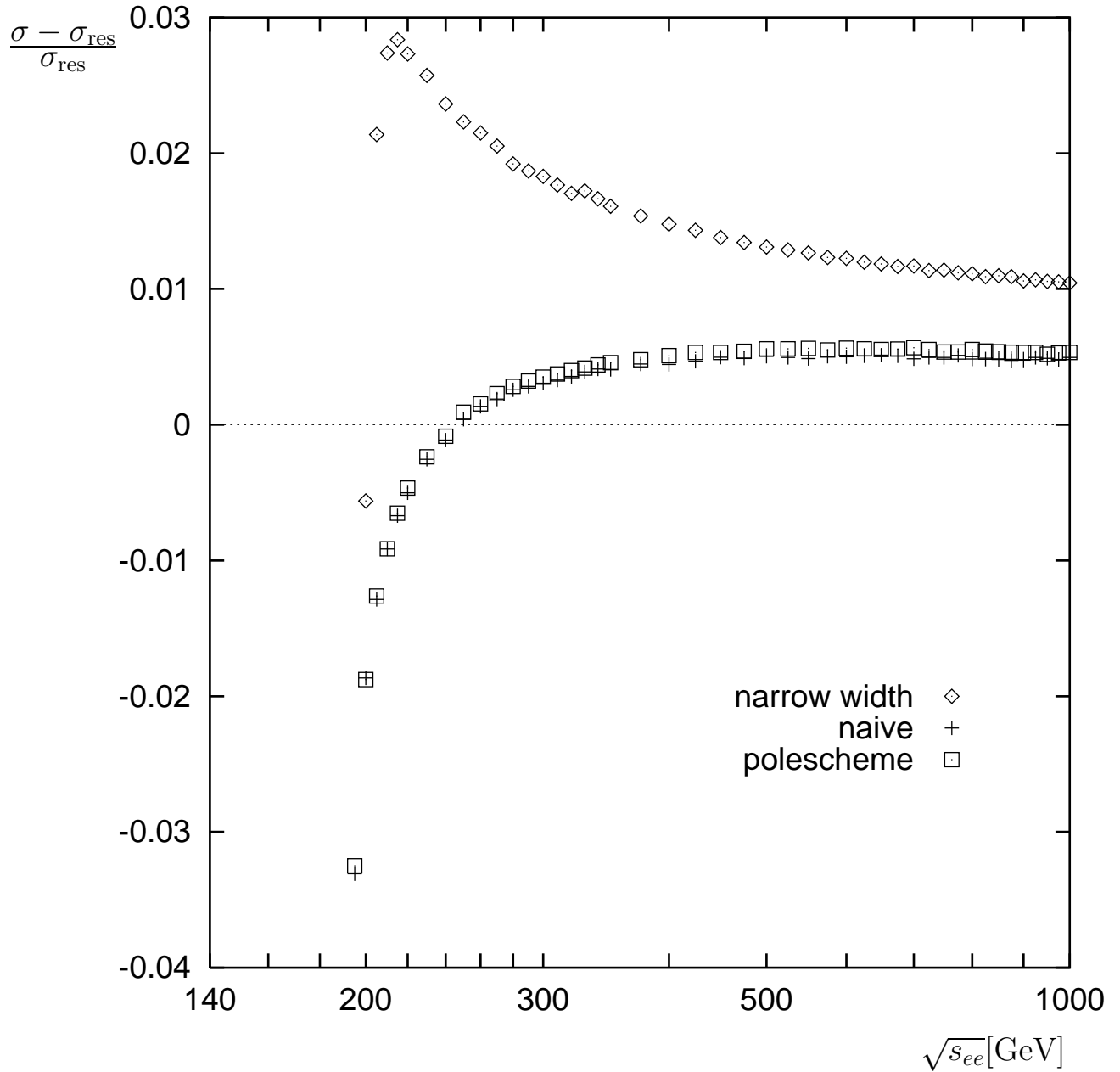


Figure 10: Relative differences with the doubly resonant cross section for  $\gamma\gamma \rightarrow \ell^- \bar{\nu}_\ell W^+$  with a realistic photon spectrum [7]. Again, the full  $\mathcal{O}(\Gamma)$  corrections, including the width of the  $W^+$ , are about twice this size.